

Title. Proteomic Characterization of Acute Kidney Injury in Patients Hospitalized with SARS-CoV2 Infection

Running Title. Proteomic Characterization of AKI in COVID-19

Authors. Ishan Paranjpe^{*1,2,19}, Pushkala Jayaraman^{*3,17,20}, Chen-Yang Su^{11,13}, Sirui Zhou^{11,12}, Steven Chen⁴, Ryan Thompson^{1†}, Diane Marie Del Valle^{1†}, Ephraim Kenigsberg^{3,4,5}, Shan Zhao⁶, Suraj Jaladanki^{1,2}, Kumardeep Chaudhary^{1,2,3}, Steven Ascolillo¹, Akhil Vaid¹, Arvind Kumar¹, Edgar Kozlova¹, Manish Paranjpe⁷, Ross O'Hagan^{1,2}, Samir Kamat¹, Faris F. Gulamali^{1,2}, Justin Kauffman^{17,19}, Hui Xie⁸, Joceyln Harris⁸, Manishkumar Patel⁸, Kimberly Argueta⁸, Craig Batchelor⁸, Kai Nie⁸, Sergio Dellepiane⁹, Leisha Scott⁸, Matthew A Levin^{1,6}, John Cijiang He⁹, Mayte Suarez-Farinas¹⁸, Steven G Coca⁹, Lili Chan⁹, Evren U Azeloglu⁹, Eric Schadt³, Noam Beckmann^{1,3}, Sacha Gnjatic¹⁰, Miram Merad⁴, Seunghee Kim-Schulze^{4,8}, Brent Richards^{11,12,14,15}, Benjamin S Glicksberg^{1,2,3}, Alexander W Charney^{1,3,11}, Girish N Nadkarni^{1,2,9,12,17,20}

*, † These authors contributed equally to the work.

Affiliations:

1. The Mount Sinai Clinical Intelligence Center (MSCIC), Icahn School of Medicine at Mount Sinai, New York, NY, USA
2. The Hasso Plattner Institute for Digital Health at Mount Sinai, Icahn School of Medicine at Mount Sinai, New York, NY, USA
3. Department of Genetics and Genomic Sciences, Icahn School of Medicine at Mount Sinai, New York, NY, USA

4. The Precision Immunology Institute, Icahn School of Medicine at Mount Sinai, New York, NY, USA.
5. Icahn Institute for Genomics and Multiscale Biology, Icahn School of Medicine at Mount Sinai, New York, NY, USA.
6. Department of Anesthesiology, Perioperative and Pain Medicine, Icahn School of Medicine at Mount Sinai, New York, New York, United States of America
7. Division of Health Sciences and Technology, Harvard Medical School, Boston, MA, USA
8. Human Immune Monitoring Center, Icahn School of Medicine at Mount Sinai, New York, NY, USA.
9. Department of Medicine, Division of Nephrology, Icahn School of Medicine at Mount Sinai, New York, New York, United States of America
10. Department of Oncological Sciences, Icahn School of Medicine at Mount Sinai, New York, NY, USA.
11. Lady Davis Institute, Jewish General Hospital, McGill University, Montréal, Québec, Canada
12. Department of Epidemiology, Biostatistics and Occupational Health, McGill University, Montréal, Québec, Canada
13. Department of Computer Science, McGill University, Montréal, Québec, Canada
14. Department of Human Genetics, McGill University, Montréal, Québec, Canada
15. Department of Twin Research, King's College London, London, United Kingdom
16. The Pamela Sklar Division of Psychiatric Genomics, Icahn School of Medicine at Mount Sinai, New York, New York, United States of America

17. The Charles Bronfman Institute for Personalized Medicine, Icahn School of Medicine
at Mount Sinai, New York, New York, United States of America

18. Department of Biostatistics, Icahn School of Medicine at Mount Sinai, New York,
New York, United States of America

19. Department of Medicine, Stanford University, San Francisco, California, United
States of America

20. Division of Data Driven and Digital Medicine (D3M), Icahn School of Medicine at
Mount Sinai, New York, New York, United States of America

***Corresponding Author:**

Girish N Nadkarni, MD

Department of Medicine, Division of Nephrology

Icahn School of Medicine at Mount Sinai, New York, NY, USA

girish.nadkarni@mountsinai.org

Abstract

Acute kidney injury (AKI) is a known complication of COVID-19 and is associated with an increased risk of in-hospital mortality. Unbiased proteomics using biological specimens can lead to improved risk stratification and discover pathophysiological mechanisms. Using measurements of ~4000 plasma proteins in two cohorts of patients hospitalized with COVID-19, we discovered and validated markers of COVID-associated AKI (stage 2 or 3) and long-term kidney dysfunction. In the discovery cohort (N= 437), we identified 413 higher plasma abundances of protein targets and 40 lower plasma abundances of protein targets associated with COVID-AKI (adjusted $p < 0.05$). Of these, 62 proteins were validated in an external cohort ($p < 0.05$, N =261). We demonstrate that COVID-AKI is associated with increased markers of tubular injury (NGAL) and myocardial injury. Using estimated glomerular filtration (eGFR) measurements taken after discharge, we also find that 25 of the 62 AKI-associated proteins are significantly associated with decreased post-discharge eGFR (adjusted $p < 0.05$). Proteins most strongly associated with decreased post-discharge eGFR included desmocollin-2, trefoil factor 3, transmembrane emp24 domain-containing protein 10, and cystatin-C indicating tubular dysfunction and injury. Using clinical and proteomic data, our results suggest that while both acute and long-term COVID-associated kidney dysfunction are associated with markers of tubular dysfunction, AKI is driven by a largely multifactorial process involving hemodynamic instability and myocardial damage.

Introduction

Severe acute respiratory syndrome coronavirus 2 (SARS-CoV-2) is a novel coronavirus that has caused the coronavirus disease 2019 (COVID-19) pandemic. Although effective vaccines are available, novel variants that may evade neutralizing antibodies exist in the population and have led to high case counts and periodic case surges. COVID-19 most commonly presents with fever, cough, and dyspnea^{1,2} and is associated with acute respiratory distress syndrome (ARDS). However, the clinical syndrome resulting from SARS-CoV-2 infection is broad, ranging from asymptomatic infection to severe disease with extrapulmonary manifestations³, including acute kidney injury⁴, acute myocardial injury^{5,6} and thrombotic complications⁷⁻¹¹. The CRIT-COV-U research group in Germany recently developed a urinary proteomics panel COV50 that could consider this variability in infection by generating biomarkers that can indicate adverse COVID-19 outcomes based on the WHO severity scale¹²

Acute kidney injury (AKI) is a particularly prominent complication. The rates of AKI vary greatly based on patient population, but evidence suggests that at least 30% of hospitalized patients and 50% of patients in the intensive care unit (ICU) develop AKI^{1,4,13-16}. Although the rate of AKI in hospitalized COVID-19 patients has decreased since the initial surge in 2020, the incidence remains high¹⁷. Like community-acquired pneumonia¹⁸, AKI is increasingly recognized as a common complication of COVID-19 in the hospitalized setting and confers significantly increased morbidity and mortality¹⁹.

There is a limited understanding of the pathophysiology of COVID-19-associated AKI. A recent paper²⁰ compared transcriptomics and proteomics of postmortem kidney samples of patients with severe COVID-19 and autopsy-derived control cohorts of

sepsis-AKI and non-sepsis-AKI. The work found common inflammatory pathways and regulatory responses including the downregulation of oxidative signaling pathways between COVID-19 AKI and sepsis-AKI. They also confirmed the observation of tubular injury in almost all their COVID-19 AKI samples while drawing similarities between the inflammation response of sepsis-associated AKI and COVID-19 associated AKI. Histopathological reports from autopsy specimens have provided conflicting insights into the pathological changes in the kidney in COVID-19. A report of 26 patients who died with COVID-19 AKI revealed acute tubular injury as a prominent mechanism²¹. Additionally, the presence of viral particles in the tubular epithelium and podocytes in autopsy specimens has been reported^{21,22}, which is evidence of direct viral invasion of the kidney. In addition, coagulopathy and endothelial dysfunction are hallmarks of COVID-19²³ and may also contribute to AKI. Finally, SARS-CoV-2 may directly activate the complement system²⁴. In addition to these mechanisms, systemic effects of critical illness (hypovolemia, mechanical ventilation) and derangements in cardiac function and volume may also contribute to COVID-19 AKI.

In addition to morbidity and mortality in the acute setting, COVID-19 is also associated with long term manifestations i.e., the post-acute sequelae of SARS-CoV2 (PASC)²⁵. Kidney function decline is a major component of PASC and a study of more than 1 million individuals found that survivors of COVID-19 had an elevated risk of post-acute eGFR decline²⁶, suggesting long term kidney dysfunction may occur following the acute infection.

Given the high incidence of COVID-19 associated kidney dysfunction, the unknown pathophysiology, and the urgent need for better approaches for risk

stratification for long term kidney function decline we aimed to characterize the proteomic changes associated with COVID associated AKI and long-term kidney function. Proteomic biomarkers have previously shown success in predicting COVID-19 outcomes²⁷⁻²⁹. Other work¹² has also applied urinary proteomic profiling to predict worsening of COVID-19 at early stages of the infection. Prior research using minimally invasive proteomics assays supports the use of peripheral serum as a readily accessible source of proteins that accurately reflect the human disease state³⁰⁻³³. We measured protein expression of more than 4000 proteins from serum samples collected in a diverse large cohort of hospitalized patients with COVID-19 and validated significant results in an independent cohort and identified proteins that are significantly different between patients with and without AKI. We then determined whether these proteomic perturbations also characterize post-discharge kidney function decline as measured by estimated glomerular filtration rate (eGFR).

MATERIALS AND METHODS

Patient cohort

An overview of the discovery cohort selection process is provided in **Fig 1**. We prospectively enrolled patients hospitalized with COVID-19 between March 24, and August 26, 2020, at five hospitals of a large urban, academic hospital system in New York City, NY into a cohort as previously described³⁴. The cohort enrolled patients who were admitted to the health care system with a COVID-19 infection and had broad inclusion criteria without specific exclusion criteria. The Mount Sinai Institutional Review Board approved this study under a regulatory approval allowing for access to patient level data and biospecimen collection³⁵. Peripheral blood specimens were collected at various points during the hospital admission for each patient.

The validation cohort included a prospective biobank from Quebec, Canada that enrolled patients hospitalized with COVID-19, as previously described²⁹. Patients were recruited from the Jewish General Hospital and Centre Hospitalier de l'Université de Montréal. Peripheral blood specimens were collected at multiple time points after admission.

We defined an AKI cohort using proteomic data acquired at the last available timepoint during the hospital course for all individuals. Patients who developed AKI after the last specimen collection timepoint were excluded. Controls were defined as individuals who developed AKI stage 1 or did not develop AKI during their hospital course.

Serum collection and Processing

Blood samples were collected in Serum Separation Tubes (SST) with a polymer gel for serum separation as previously described³⁵. Samples were centrifuged at 1200 g for 10 minutes at 20°C. After centrifugation, serum was pipetted to a 15 mL conical tube. Serum was then aliquoted into cryovials and stored at -80°C.

Definition of Acute Kidney Injury

We defined AKI (stage 2 or 3) as per Kidney Disease Improving Global Outcomes (KDIGO) criteria: an increase in serum creatinine of at least 2.0 times the baseline creatinine³⁶. For patients with previous serum creatinine measurement available in the 365 days prior to admission, the minimum value in this period was considered the baseline creatinine. For patients without a baseline creatinine in this period, a baseline value was calculated based on an estimated glomerular filtration rate (eGFR) of 75 ml/min per 1.73 m² as per the KDIGO AKI guidelines.

Clinical data collection

We collected demographic and laboratory data collected as part of standard medical care from an institutional electronic health record (EHR) database. We defined clinical comorbidities using diagnostic codes recorded in the EHR before the current hospital admission. To account for disease severity at the time of specimen collection, we defined supplemental oxygen requirement as 0 if the patient was not receiving supplemental oxygenation or on nasal cannula, 1 if the patient was receiving non-invasive mechanical ventilation (CPAP, BIPAP), or 2 if the person was receiving invasive mechanical ventilation.

Somalogic proteomic assay

We used the *SomaScan* discovery platform to quantify levels of protein expression. The *SomaScan* platform is a highly multiplexed aptamer based proteomic assay based on Slow Off-rate Modified single-stranded DNA Aptamers (SOMAMers) capable of simultaneously detecting 4497 proteins in biological samples in the form of relative fluorescent units (RFUs). The assay was run using the standard 12 hybridization normalization control sequences to assess for variability in the Agilent plate quantification process, five human calibrator control pooled replicates, and 3 quality control pooled replicates to control for batch effects. Standard preprocessing protocols were applied as per Somalogic's guidelines published previously³⁷ The specificity and stability of the SOMAScan assay has been described previously³⁸ Briefly, the data was first normalized using the 12 hybridization controls to remove hybridization variation within a run. Then, median signal normalization is performed with calibrator samples across plates to remove variation in sample-to-sample differences attributable to variations due to pipetting, reagent concentrations, assay timings and other technical aspects. Data was then calibrated to remove assay differences between runs. Standard Somalogic acceptance criteria for quality control metrics were used (plate scale factor between 0.4 and 2.5 and 85% of QC ratios between 0.8 and 1.2). Samples with intrinsic issues such as reddish appearance or low sample volume were also removed as part of the Somalogic quality control protocol. After quality control and normalization procedures, the resulting relative fluorescence unit (RFU) values were log₂ transformed.

Dimensionality reduction

Principal component analysis (PCA) was performed using log₂ transformed RFU values of all proteins. Pairwise plots of the top three principal components were plotted.

Differential expression analysis for prevalent AKI

Using data from the AKI cohort, log₂ transformed normalized protein values were modelled using multivariable linear regression in the Limma framework³⁹. Models were adjusted for age, sex, history of chronic kidney disease (CKD), and supplemental oxygen requirement (0, 1, or 2 [see above]) at the time of specimen collection. P-values were adjusted using the Benjamin-Hochberg procedure to control the false discovery rate (FDR) at 5%.

Proteins associated with change in creatinine

Similarly, we also computed the maximum change in creatinine during hospitalization from baseline for each individual in the discovery cohort. We then associated protein expression values measured at the last available timepoints with maximal change in creatinine to identify a dose response relationship. Models were adjusted for age, sex, history of chronic kidney disease (CKD), and supplemental oxygen requirement (0, 1, or 2 [see above]) at the time of specimen collection.

Proteomic characterization of long-term kidney function in discovery cohort

Outpatient creatinine values measured after discharge were used to compute estimated glomerular filtration rate (eGFR) values the CKD-EPI equation. All values were taken from the EHR as part of routine clinical care with follow-up until 12/2/2021.

To determine whether AKI associated protein expression correlated with post-discharge kidney function, we fit a mixed effects linear regression model with random intercept . Using the discovery cohort, protein expression of AKI-associated proteins measured at the last available timepoint during admission was used. The dependent variable was eGFR and the model was adjusted for age, sex, baseline creatinine, history of CKD, maximum AKI stage during the hospital admission, and day of eGFR measurement after hospital discharge. Models included a random effect of patient ID to adjust for correlation between eGFR values taken from the same individuals. Significance was evaluated using a t-test with Satterthwaite degrees of freedom implemented in the lmerTest R package⁴⁰. P values were adjusted using the Benjamin-Hochberg procedure to control the false discovery rate (FDR) at 5%.

We then plotted the post-discharge eGFR values over time for individuals separated by protein expression tertiles (bottom 33rd percentile, middle 33th percentile, and top 33th percentile). We transformed data using the LOESS smoothing function as implemented in the ggplot R package.

Data analysis and visualization

We performed all statistical analysis using R version 4.0.3. Protein-protein interaction (PPI) network was constructed using the Network X package in Python v3.4.10 to display a Minimum Spanning Tree (MST) using Prim's algorithm. Network clustering was conducted using the MCL cluster algorithm and functional enrichment was carried out using the STRING⁴¹ database in Cytoscape⁴². Using results from a recent publication³⁰, we also annotated protein quantitative trait loci (pQTLs) for the set of COVID AKI-associated

proteins. For each AKI-associated protein, we determined whether or not cis and trans pQTL associations had been reported.

Data and Code Availability

Data is available by contacting the senior author, Girish Nadkarni (girish.nadkarni@mountsinai.org).

Code is available at https://github.com/Nadkarni-Lab/aki_covid_proteomics

RESULTS

Discovery and Validation Cohort Overview

To discover proteins associated with COVID-AKI, we enrolled a prospective cohort of patients hospitalized with COVID-19 admitted between March 24, 2020 and August 26, 2020 into a biobank as previously described³⁴. Cases were defined as patients who developed AKI (stage 2 or 3) during their hospital admission and controls included all other patients (**Fig 1**). Characteristics of cases and controls in the discovery cohort are provided in **Table 1**. Patients who developed AKI were significantly older (67 vs. 60 years, $p < 0.001$), more commonly Hispanic/Latino (48% vs 37%, $p = 0.012$), and had a greater prevalence of atrial fibrillation (17% vs 8%, $p = 0.008$), diabetes (37% vs 20%, $p < 0.001$), and chronic kidney disease (20% vs 4%, $p < 0.001$). We then validated these associations in an external cohort from Quebec, Canada. Characteristics of the validation cohort are provided in **Supplementary Table 1**. In the validation cohort, compared to controls, AKI (stage 2 or 3) cases had a significantly higher prevalence of CKD (29% vs 11%, $p = 0.01$) and a higher rate of intubation at the time of blood draw (49% vs 13%).

Identification of proteins associated with prevalent AKI

In the discovery cohort, serum levels of 4496 proteins were quantified using the *SomaScan* platform using samples collected at multiple timepoints during the hospital course (**Supplementary Table 2**) as previously described³⁴. We first identified proteins associated with prevalent AKI using measurements taken after the onset of AKI in cases and the last available measurement in controls (**Fig 1**, 71 cases and 366 controls). The top three principal components (PCs) distinctly separate samples by case status (**Fig 2A**). We fit a multivariable linear regression model for the log₂ normalized protein expressions adjusted for age, sex, history of chronic kidney disease (CKD), and maximum oxygen requirement at the time of blood draw. We identified 413 proteins with higher plasma abundances and 30 proteins with lower plasma abundance (**Supplementary Table 3**).

Validation of AKI-associated proteins

We then performed an external validation of AKI-associated proteins in a prospective biobank cohort from Quebec, Canada. Of the 443 proteins significantly associated with AKI in the discovery cohort (FDR adjusted $P < 0.05$), 62 were also associated with AKI in the validation cohort ($p < 0.05$, **Table 2**). All validated proteins were associated with an increased risk of AKI. The fold changes of validated proteins in the discovery and validation cohort were highly correlated with a Pearson correlation of 0.71 (**Fig 2B**). The 62-protein signature distinctly separated AKI cases from cohorts in the discovery cohort (**Fig 2C**). Using reported plasma pQTL associations from a recent publication, of the 62 AKI associated proteins, 45 had both cis and trans pQTLs, 14 had only trans pQTLs, and 2 had cis pQTLs (Supplementary Figure 1). Protein-protein

interaction (PPI) network analysis revealed enrichment of several highly connected proteins, including LCN2 (alternative name: NGAL), REG3A, and MB (**Fig 4A**). The AKI-associated protein network also included a cluster of cardiac structural proteins (**Fig 4B**), TNNT2, TTN, MYL3, SRL, and NPPB (alternative name: BNP).

Proteins associated with change in creatinine:

We then tried to identify which AKI-associated proteins demonstrated a dose dependent relationship with change in creatinine. Using the discovery dataset, we fit a multivariable linear regression model for maximal change in creatinine during hospitalization and found that all 62 AKI-associated proteins were also significantly associated with maximal change in creatinine ($P < 0.05$, Supplementary Table 4).

Proteomic characterization of post-acute kidney dysfunction

Given the previously reported association of COVID-19 AKI with long-term eGFR decline⁴³, we hypothesized that significant proteomic markers associated with COVID-19 AKI are also associated with post-discharge eGFR. We included all outpatient eGFR measurements taken after discharge from patients in the Mount Sinai biobank cohort. Of the 437 patients in the cohort, 181 patients had at least one outpatient post-discharge eGFR measurement. The median number of eGFR measurements was 4 with an interquartile of 9. The first post-discharge eGFR was measured at a median of 37 days after discharge. The last post-discharge eGFR was measured at a median of 374 days after discharge (Supplementary Figure 2).

We used a mixed effects linear model accounting for baseline creatinine, AKI stage during the COVID admission and repeated eGFR measurements to associate the 62 protein AKI signature with long-term eGFR. Of the 62 AKI-associated proteins, 25

were significantly (FDR adjusted $P < 0.05$) associated with long-term post-discharge eGFR (**Fig 3, Fig 5A**). All 25 eGFR-associated proteins were negatively correlated with post-discharge eGFR (**Table 3**). However, the strength of association with AKI was not significantly associated with the strength of association with post-discharge eGFR. Proteins most strongly associated (by P value) with decreased post-discharge eGFR included desmocollin-2, trefoil factor 3, transmembrane emp24 domain-containing protein 10, and cystatin-C (**Fig 5B**).

DISCUSSION

Using proteomic profiling in two large groups of patients hospitalized with COVID-19, we report several observations. First, we identified specific protein markers of AKI and post-discharge kidney dysfunction, both well-documented sequelae of COVID-19^{4,43}. Second, in the acute phase, tubular injury and hemodynamic perturbation may play a role. Thus, characterization of the peripheral blood suggests specific large-scale perturbations of the proteome that accompany both AKI and long-term eGFR decline with implications for more specific prognostic models and targeted therapeutic development.

Based on our results, we hypothesize that COVID AKI may involve several mechanisms: tubular injury, neutrophil activation, and hemodynamic perturbation. First, we found significantly higher plasma abundances of NGAL (LCN2), a canonical marker of tubular injury that is also involved in neutrophil activation. NGAL is secreted by circulating neutrophils and kidney tubular epithelium in response to systemic

inflammation or ischemia. Since renal tubular epithelial cells express the angiotensin-converting enzyme 2 (ACE2) receptor which enables SARS-CoV2 viral entry into cells, direct tubular infection may cause the release of NGAL into the serum and urine. This potential mechanism is supported by our results and remains a testable hypothesis.

Although NGAL is a known marker for intrinsic AKI accompanied by tubular injury, it is relatively insensitive to pre-renal AKI caused by hemodynamic disturbance^{44,45}.

However, our results demonstrate higher plasma abundance of BNP, a protein released in the setting of volume overload as well as several cardiac structural proteins (cardiac troponin T, titin, myosin light chain 1, and sarcalumenin). This proteomic signature may represent an impaired crosstalk between the cardiovascular system and kidney in which myocardial injury leads to decreased renal perfusion and eventual AKI. Myocardial injury has been previously reported in patients hospitalized with COVID-19⁶ and thus may contribute to the multifactorial nature of COVID-AKI. It is worth noting that in addition to myocardial injury, BNP may also be increased in critical illness due to pro-inflammatory cytokine release.

Since COVID-AKI increases the risk of long-term eGFR decline⁴³, we then sought to determine whether these two phenomena shared common proteomic markers. Surprisingly, we found that although almost half of the AKI-associated proteins were also significantly associated with post-discharge eGFR decline, the strengths of associations were not correlated. While COVID-AKI is likely caused by a combination of intrinsic tubular injury and hemodynamic disturbance in the setting of critical illness, long term eGFR decline was associated with increased expression of trefoil factor 3 (TFF3),

a known prognostic marker for incident CKD⁴⁶. Trefoil factors are a class of small peptides expressed in colonic and urinary tract epithelia that play essential roles in regeneration and repair of epithelial tissue^{47,48}. Immunohistochemistry reveals TFF3 expression is localized to the tubular epithelial cells in kidney specimens from patients with CKD⁴⁶, suggesting that long term eGFR decline may be associated with renal tubular epithelial damage. The exact pathological role of TFF3 in the renal tubules is unclear but it has been hypothesized to play a role in repair of kidney damage⁴⁹. Additionally, TFF3 release from the renal interstitium has also been hypothesized to direct the epithelial-to-mesenchymal transition (EMT) in renal interstitial fibrosis, a main pathway that leads to ESKD⁴⁶. Our results implicate tubular damage in both AKI and long term eGFR decline suggesting that SARS-CoV2 may preferentially target this region of the nephron. While AKI in the acute setting may be a result of ischemia and decreased renal perfusion associated with critical illness, the specific elevation of TFF3 associated with eGFR decline implicates a more general pattern of tubular injury that underlies COVID mediated kidney dysfunction. Since the ACE2, is preferentially expressed in the tubular epithelial cells of the kidney^{50,51}, the elevation of markers of tubular damage in the plasma may represent direct viral invasion of tubular epithelia cells. However, again this would need to be tested using biopsy/autopsy specimens or other mechanistic studies. Direct viral entry into the kidney remains controversial and using our current data we are not able to comment on this mechanism.

Our study should be interpreted in the context of certain limitations. First, samples were collected during the hospital course of patients with confirmed COVID-19. However, the timepoints were not systematic due to logistical challenges during the

peak of the COVID-19 pandemic and thus are not standardized between patients. Since a subset of patients had AKI at the time of admission, these patients were excluded from our analysis since specimens were collected after admission. Additionally, we did not include patients who developed AKI without COVID and were unable to determine whether COVID-AKI has unique proteomic markers compared to other forms of sepsis-AKI. Thus, our AKI cases may be biased towards less severe presentations. Second, since kidney injury is usually not an isolated phenomenon in critically ill patients, the protein expression changes observed may have been partially due to damage to other organs, such as the lung, liver, and heart. However, we accounted for non-kidney damage by adjusting for the highest level of ventilatory support and thus our results are likely a reflection of kidney injury. However, our results do show the importance of crosstalk between the cardiac system and the kidneys. Additionally, we did not include proteomic measurements from urine specimens and thus it is unclear whether poor filtration or resorption of proteins plays a role in peripheral blood protein concentrations. For example, poor resorption of cystatin-C in the setting of AKI may have led to the increased peripheral blood cystatin-C that we report. Our study was adequately powered to detect effect sizes of greater than or equal to 1.6. Additionally, since we enrolled patients only from March-October 2020, we cannot generalize our findings to other COVID-19 variants and time periods. Although we adjusted our regression models for history of CKD, it is possible that unmeasured confounding due to preexisting impaired kidney function has not completely been controlled for in our analyses. Finally, our cohort did not include autopsy or kidney biopsy specimens. Histopathological

analysis of kidney specimens is necessary to determine the mechanism of AKI and whether viral particles are present in the kidney.

In conclusion, we provide the first comprehensive characterization of the plasma proteome of AKI and long term eGFR decline in hospitalized COVID-19 patients. Our results suggest in the setting of COVID-AKI and post-discharge kidney dysfunction there is evidence of tubular damage in the peripheral blood but that in the acute setting, several factors including hemodynamic disturbance and myocardial injury also play a role.

Author contributions:

Conceptualization: IP, GNN, AWC, SZ, NB, ES, EK, LC, SC, BM, SD
Methodology: IP, PJ, RT, KC, SA, AV, SJ, MP, RO, SK, SZ, EUA, FFG, MSF
Investigation: IP, PJ, RT, EK, SZ, SJ, KC, AK, SG, HX, JH, MP, KA, CB, KN, RO
Visualization: IP, PJ
Funding acquisition: GNN, AWC, BSG, MM, NB
Supervision: GNN, AWC, BSG, MM, SK, NB, ES, JCH
Writing: IP, PJ, GNN, SK

Acknowledgements: We would like to thank the scientists at Somalogic for their assistance with technical and scientific questions about the assay.

Disclosures: GNN and SGC reports grants, personal fees, and non-financial support from Renalytix. GNN reports non-financial support from Pensieve Health, personal fees from AstraZeneca, personal fees from BioVie, personal fees from GLG Consulting, personal fees from Siemens Healthineers from outside the submitted work. IP receives personal fees from Character Biosciences.

Funding: EUA, GNN, JCH and SGC are partially funded by R01 DK118222. GNN also is supported by R01DK127139, R01HL155915 and R56DK126930.

Figure Captions

Fig 1: Overview of the discovery cohort selection process.

Fig 2: **A.** Top 3 Principal Components show separation of the sample by AKI (stage 2 or 3) case status. **B.** External validation of AKI associated proteins in the discovery cohort shows high correlation with increased risk of AKI with significance of $p < 0.05$. **C.** Expression heatmap shows a distinct separation of the cases and controls using the 62 significant proteins identified from the validation cohort in the discovery cohort.

Fig 3: Nested Venn diagram of the analyses performed.

Fig 4: **A.** Protein–protein interaction (PPI) network (Minimum Spanning Tree) of the 62 overlapping AKI associated proteins with a score > 0.4 . The size of each node corresponds to number of interactions and the thickness of the edges represent the weight of the interactions between the nodes. **B.** MCL algorithm was used to identify tightly connected cluster of proteins which was functionally enriched for cardiac structure proteins using the STRING database.

Fig 5: Proteomic characterization of long-term eGFR decline. **A.** Comparison of strengths of association with AKI and long term eGFR for proteins associated with AKI in both the discovery and validation cohorts. **B.** Trend in eGFR values separated by protein expression for tertiles for proteins most significantly (by P value) associated with eGFR trend.

Tables

Table 1: Demographic and clinical comorbidities of patients hospitalized with COVID-19 in the discovery cohort separated by the development of AKI (stage 2 or 3) during their hospital course.

Characteristic	Developed AKI (stage 2 or 3) during hospitalization (N = 73)	AKI stage 1 or no AKI during hospitalization (N = 366)	P Value
Age, mean (SD)	63 (14.7)	61.8 (18.2)	0.8
Male, n (%)	46 (65%)	218 (60%)	0.43
Race, n (%)			0.74
Caucasian	23 (32%)	136 (37%)	
Black	17 (24%)	81 (22%)	
Other	31 (44%)	149 (41%)	
Ethnicity, n (%)			0.23
Hispanic	34 (48%)	144 (39%)	
Not Hispanic or Latino	37 (52%)	213 (58%)	
Unknown / Not Reported	0 (0%)	9 (2%)	
Comorbidities, n (%)			
Atrial Fibrillation	9 (13%)	38 (10%)	0.53
Coronary Artery Disease	10 (14%)	50 (14%)	1
Arterial Hypertension	30 (42%)	142 (39%)	0.6
Diabetes	30 (42%)	81 (22%)	<0.001
Chronic Kidney Disease	22 (31%)	20 (5%)	<0.001
Highest respiratory support, n (%)			<0.001
Intubation	33 (46%)	39 (11%)	
Non-invasive ventilation (CPAP, BIPAP, high-flow cannula)	3 (4%)	19 (5%)	
Nasal cannula	21 (30%)	184 (50%)	
None of the above	14 (20%)	124 (34%)	
Vitals and Laboratory parameters during hospitalization, mean (standard deviation)			
Minimum systolic blood pressure (mmHg)	104 (15.7)	110 (14.9)	<0.001
Maximum pulse (bpm)	106 (20.2)	93.9 (18.3)	<0.001

Maximum blood urea nitrogen (mmol/L)	53 (34)	17 (11)	<0.001
Maximum creatinine (mg/dL)	4.04 (2.94)	0.945 (0.51)	<0.001
Maximum white blood cell count (10 ⁹ /L)	12.9 (8.07)	8.83 (5.35)	<0.001
Minimum platelet count (10 ⁹ /L)	14 (20%)	124 (34%)	<0.001
Max ferritin (ug/L)	2210 (2540)	1030 (1310)	<0.001
Max lactate (mmol/L)	1.98 (1.54)	1.5 (0.617)	0.65
Vasopressor use during hospitalization, n (%)			
Any vasopressor	34 (48%)	50 (14%)	<0.001
Norepinephrine	32 (45%)	42 (11%)	<0.001
Vasopressin	17 (24%)	8 (2%)	<0.001
Phenylephrine	10 (14%)	8 (2%)	<0.001
Epinephrine	2 (3%)	6 (2%)	0.62
Milrinone	3 (4%)	2 (1%)	0.03
Dopamine	1 (1%)	1 (0%)	0.3

Table 2: Validation of AKI-associated proteins. Strength of association of proteins significantly associated with AKI (stage 2 or 3) in both the discovery (adjusted P <0.05) and validation cohort (P <0.05) are provided. Significance was determined by fitting a linear model adjusted for age, sex, history of CKD, and maximum oxygen requirement at the time of blood draw.

Gene Name	Gene Symbol	Discovery cohort				Validation cohort		
		logF C	Fold Change	P	FDR	LogF C	Fold Change	P
Trypsin-2	PRSS2	1.98	3.94	3.16E-26	1.42E-22	1.41	2.65	0.0019
Lithostathine-1-alpha	REG1A	2.07	4.20	9.23E-38	4.15E-34	1.36	2.56	0.0076
Peroxidasin homolog	PXDN	1.97	3.93	1.39E-34	6.25E-31	1.26	2.39	0.0047
Regenerating islet-derived protein 3-alpha	REG3A	1.84	3.59	6.44E-26	2.90E-22	1.26	2.39	0.0139
Ribonuclease pancreatic	RNASE1	2.38	5.22	1.53E-38	6.87E-35	1.21	2.31	0.0021
Trefoil factor 3	TFF3	1.68	3.21	2.13E-41	9.55E-38	1.16	2.24	0.0238
Adapter molecule crk	CRK	1.00	1.99	8.67E-18	3.90E-14	1.15	2.22	0.0219
Tumor necrosis factor receptor superfamily member 1A	TNFRSF1A	1.15	2.22	3.86E-21	1.74E-17	1.15	2.22	0.0281
Trefoil factor 2	TFF2	1.20	2.30	3.36E-16	1.51E-12	1.12	2.18	0.0273
Fatty acid-binding protein, heart	FABP3	1.28	2.42	3.09E-21	1.39E-17	1.11	2.17	0.0356
Copper transport protein ATOX1	ATOX1	1.57	2.96	2.04E-40	9.16E-37	1.11	2.16	0.0072
Angiopietin-2	ANGPT2	1.15	2.23	1.44E-08	6.45E-05	1.11	2.16	0.0342

Inactive pancreatic lipase-related protein 1	PNLIPRP1	1.28	2.42	5.64E-15	2.54E-11	1.10	2.15	0.0296
Trypsin-3	PRSS3	1.32	2.50	9.07E-18	4.08E-14	1.09	2.13	0.0069
Acyl-CoA-binding protein	DBI	1.46	2.74	1.82E-44	8.20E-41	1.08	2.12	0.0360
Ganglioside GM2 activator	GM2A	1.24	2.37	2.02E-40	9.09E-37	1.08	2.11	0.0088
Neuroblastoma suppressor of tumorigenicity 1	NBL1	1.53	2.89	1.79E-37	8.03E-34	1.08	2.11	0.0099
Apolipoprotein F	APOF	1.07	2.10	2.97E-14	1.34E-10	1.07	2.10	0.0317
Collagen alpha-1(XXVIII) chain	COL28A1	1.29	2.44	2.29E-34	1.03E-30	1.06	2.09	0.0252
Carbonic anhydrase 3	CA3	1.31	2.49	2.13E-13	9.58E-10	1.06	2.08	0.0174
CD59 glycoprotein	CD59	1.09	2.12	5.67E-21	2.55E-17	1.04	2.06	0.0318
Ephrin-B2	EFNB2	0.99	1.99	1.45E-14	6.52E-11	1.04	2.06	0.0437
Transmembrane emp24 domain-containing protein 10	TMED10	1.37	2.59	2.39E-42	1.07E-38	1.03	2.05	0.0078
Trypsin-1	PRSS1	1.07	2.10	3.15E-13	1.42E-09	1.03	2.04	0.0456
Cystatin-D	CST5	1.11	2.16	4.02E-13	1.81E-09	1.02	2.03	0.0464
Transgelin	TAGLN	1.16	2.24	1.60E-27	7.20E-24	1.01	2.02	0.0379
Myosin light chain 3	MYL3	1.82	3.54	2.12E-15	9.54E-12	1.01	2.01	0.0127
IGF-like family receptor 1	IGFLR1	1.46	2.75	1.97E-26	8.85E-23	1.00	2.00	0.0242
Small ubiquitin-related modifier 2	SUMO2	1.69	3.24	2.07E-44	9.29E-41	0.98	1.97	0.0469
Tyrosine-protein kinase transmembrane receptor ROR2	ROR2	1.39	2.62	1.29E-32	5.82E-29	0.97	1.96	0.0410

Troponin T, cardiac muscle	TNNT2	1.61	3.06	6.66E-27	2.99E-23	0.96	1.95	0.0233
Complexin-2	CPLX2	1.36	2.57	5.43E-30	2.44E-26	0.94	1.92	0.0145
Serine protease inhibitor Kazal-type 7	SPINK7	0.87	1.83	4.06E-18	1.82E-14	0.94	1.91	0.0242
Myoglobin	MB	1.45	2.73	7.19E-23	3.23E-19	0.93	1.91	0.0427
Cystatin-C	CST3	1.19	2.28	2.09E-41	9.38E-38	0.93	1.91	0.0297
Hepatoma-derived growth factor	HDGF	0.41	1.33	4.05E-07	1.82E-03	0.93	1.90	0.0241
Ig gamma-4, Kappa	IGHG4	0.65	1.57	2.26E-12	1.02E-08	0.92	1.90	0.0217
Desmocollin-2	DSC2	1.26	2.40	2.84E-39	1.28E-35	0.91	1.88	0.0249
PILR alpha-associated neural protein	PIANP	0.87	1.83	1.47E-24	6.60E-21	0.91	1.88	0.0226
Ephrin type-A receptor 2	EPHA2	1.04	2.05	1.72E-21	7.74E-18	0.91	1.87	0.0294
Natriuretic peptides B	NPPB	0.69	1.61	8.76E-09	3.94E-05	0.90	1.87	0.0399
Chymotrypsinogen B	CTRB1	1.00	2.00	1.62E-09	7.29E-06	0.90	1.86	0.0202
Secretogranin-1	CHGB	1.36	2.57	2.28E-37	1.02E-33	0.89	1.86	0.0180
Ephrin-B1	EFNB1	0.89	1.86	1.30E-38	5.86E-35	0.89	1.85	0.0365
Parathyroid hormone	PTH	1.05	2.07	2.68E-14	1.20E-10	0.88	1.84	0.0443
Bola-like protein 1	BOLA1	0.78	1.72	1.61E-29	7.26E-26	0.87	1.83	0.0288
Serine/threonine-protein kinase receptor R3	ACVRL1	1.00	1.99	9.51E-32	4.28E-28	0.87	1.83	0.0200
Tumor necrosis factor receptor superfamily member 19	TNFRSF19	1.06	2.08	1.84E-33	8.29E-30	0.87	1.83	0.0272

Ribonuclease K6	RNASE6	1.18	2.26	9.28E-29	4.17E-25	0.87	1.83	0.0498
Selenoprotein W	SEPW1	1.26	2.40	1.56E-15	7.01E-12	0.86	1.82	0.0489
Protein delta homolog 2	DLK2	1.02	2.02	2.29E-15	1.03E-11	0.86	1.81	0.0415
Asialoglycoprotein receptor 1	ASGR1	0.91	1.88	5.36E-13	2.41E-09	0.85	1.80	0.0434
Matrix-remodeling-associated protein 7	MXRA7	0.73	1.66	7.02E-22	3.15E-18	0.84	1.80	0.0288
Neutrophil gelatinase-associated lipocalin	LCN2	1.13	2.19	6.27E-22	2.82E-18	0.84	1.79	0.0363
Osteopontin	SPP1	1.11	2.16	4.47E-21	2.01E-17	0.82	1.77	0.0370
Protocadherin gamma-A10	PCDHGA10	0.90	1.87	5.70E-16	2.56E-12	0.81	1.76	0.0406
DnaJ homolog subfamily B member 12	DNAJB12	0.94	1.91	9.54E-17	4.29E-13	0.81	1.75	0.0466
Sarcalumenin	SRL	1.02	2.02	6.00E-38	2.70E-34	0.80	1.74	0.0475
Discoidin domain-containing receptor 2	DDR2	1.07	2.10	3.40E-21	1.53E-17	0.78	1.71	0.0359
Titin	TTN	1.22	2.33	5.42E-25	2.44E-21	0.77	1.71	0.0281
Colipase	CLPS	0.86	1.82	1.95E-17	8.77E-14	0.75	1.68	0.0362
Stathmin-3	STMN3	0.37	1.29	6.95E-09	3.13E-05	0.74	1.67	0.0480

Table 3: Association of AKI-associated proteins with post-discharge eGFR. A mixed effects linear model adjusted for age, sex, history of CKD, baseline creatinine, AKI stage during the COVID admission and number repeated eGFR measurements was fit. Proteins significantly associated with eGFR (adjusted P <0.05) are provided.

Gene name	Coefficient	P Value	Adjusted P Value	Uniprot ID
BolA-like protein 1	-18.022031	1.38x10 ⁻⁵	0.0008	Q9Y3E2
Cystatin-C	-17.63355	3.40x10 ⁻⁷	2.14x10 ⁻⁵	P01034
Desmocollin-2	-16.597692	1.63x10 ⁻⁹	1.03 x 10 ⁻⁷	Q02487
Transmembrane emp24 domain-containing protein 10	-15.819807	1.36x10 ⁻⁸	8.54x10 ⁻⁷	P49755
Ephrin-B1	-15.167647	0.0002	0.01	P98172
Serine/threonine-protein kinase receptor R3	-13.939695	7.64x10 ⁻⁵	0.004	P37023
Ganglioside GM2 activator	-13.060806	1.17x10 ⁻⁵	0.0007	P17900
Matrix-remodeling-associated protein 7	-11.88046	0.0002	0.017	P84157
PILR alpha-associated neural protein	-11.803896	3.23x10 ⁻⁵	0.002	Q8IYJ0
Trefoil factor 3	-11.738116	1.60x10 ⁻⁸	1.01x10 ⁻⁶	Q07654
Copper transport protein ATOX1	-11.216693	4.38x10 ⁻⁶	0.0002	O00244
Serine protease inhibitor Kazal-type 7	-11.157036	5.77x10 ⁻⁶	0.0003	P58062
IGF-like family receptor 1	-11.007485	4.79x10 ⁻⁷	3.02x10 ⁻⁵	Q9H665
Complexin-2	-10.73936	1.33x10 ⁻⁶	8.36 x 10 ⁻⁵	Q6PUV4
Collagen alpha-1(XXVIII) chain	-10.047217	0.0001	0.006	Q2UY09
CD59 glycoprotein	-9.9917438	1.74x10 ⁻⁵	0.001	P13987
Ribonuclease K6	-9.9898356	0.0001	0.006	Q93091
Transgelin	-9.9393974	0.0001	0.01	Q01995
DnaJ homolog subfamily B member 12	-8.2638876	0.0004	0.03	Q9NXW2
Protein delta homolog 2	-7.7406286	0.0002	0.01	Q6UY11
Discoidin domain-containing receptor 2	-7.6524963	0.0006	0.04	Q16832
Ribonuclease pancreatic	-7.40997	8.01x10 ⁻⁷	5.05x10 ⁻⁵	P07998
Ephrin-B2	-7.2943084	0.0001	0.009	P52799
Peroxidasin homolog	-7.2282085	1.75x10 ⁻⁵	0.001	Q92626
Trefoil factor 2	-7.2179491	1.2x10 ⁻⁵	0.0007	Q03403

References.

1. Richardson S, Hirsch JS, Narasimhan M, et al. Presenting Characteristics, Comorbidities, and Outcomes among 5700 Patients Hospitalized with COVID-19 in the New York City Area. *JAMA - J Am Med Assoc* 2020;
2. Goyal P, Choi JJ, Pinheiro LC, et al. Clinical characteristics of COVID-19 in New York City. *N. Engl. J. Med.* 2020;
3. Gupta A, Madhavan M V., Sehgal K, et al. Extrapulmonary manifestations of COVID-19. *Nat. Med.* 2020;
4. Chan L, Chaudhary K, Saha A, et al. AKI in Hospitalized Patients with COVID-19. *J Am Soc Nephrol [Internet]* 2020;ASN.2020050615. Available from: <http://jasn.asnjournals.org/content/early/2020/09/02/ASN.2020050615.abstract>
5. Sala S, Peretto G, Gramegna M, et al. Acute myocarditis presenting as a reverse Tako-Tsubo syndrome in a patient with SARS-CoV-2 respiratory infection. *Eur. Heart J.* 2020;
6. Lala A, Johnson KW, Januzzi JL, et al. Prevalence and Impact of Myocardial Injury in Patients Hospitalized With COVID-19 Infection. *J Am Coll Cardiol* 2020;76(5):533–46.
7. Cui S, Chen S, Li X, Liu S, Wang F. Prevalence of venous thromboembolism in patients with severe novel coronavirus pneumonia. *J Thromb Haemost* 2020;
8. Bilaloglu S, Aphinyanaphongs Y, Jones S, Iturrate E, Hochman J, Berger JS. Thrombosis in Hospitalized Patients with COVID-19 in a New York City Health System. *JAMA - J. Am. Med. Assoc.* 2020;
9. Lodigiani C, Iapichino G, Carengo L, et al. Venous and arterial thromboembolic

- complications in COVID-19 patients admitted to an academic hospital in Milan, Italy. *Thromb Res* 2020;
10. Helms J, Tacquard C, Severac F, et al. High risk of thrombosis in patients with severe SARS-CoV-2 infection: a multicenter prospective cohort study. *Intensive Care Med* 2020;
 11. Paranjpe I, Fuster V, Lala A, et al. Association of Treatment Dose Anticoagulation With In-Hospital Survival Among Hospitalized Patients With COVID-19. *J. Am. Coll. Cardiol.* 2020;
 12. Wendt R, Thijs L, Kalbitz S, et al. A urinary peptidomic profile predicts outcome in SARS-CoV-2-infected patients. *eClinicalMedicine* 2021;
 13. Zhou F, Yu T, Du R, et al. Clinical course and risk factors for mortality of adult inpatients with COVID-19 in Wuhan, China: a retrospective cohort study. *Lancet* 2020;
 14. Argenzian MG, Bruc SL, Slate CL, et al. Characterization and clinical course of 1000 patients with coronavirus disease 2019 in New York: Retrospective case series. *BMJ* 2020;
 15. Mohamed MMB, Lukitsch I, Torres-Ortiz AE, et al. Acute Kidney Injury Associated with Coronavirus Disease 2019 in Urban New Orleans. *Kidney360* 2020;
 16. Cao J, Tu WJ, Cheng W, et al. Clinical features and short-term outcomes of 102 patients with coronavirus disease 2019 in Wuhan, China. *Clin Infect Dis* 2020;
 17. Dellepiane S, Vaid A, Jaladanki SK, et al. Acute Kidney Injury in Patients Hospitalized With COVID-19 in New York City: Temporal Trends From March 2020 to April 2021. *Kidney Med* 2021;

18. Murugan R, Karajala-Subramanyam V, Lee M, et al. Acute kidney injury in non-severe pneumonia is associated with an increased immune response and lower survival. *Kidney Int* 2010;
19. Nadim MK, Forni LG, Mehta RL, et al. COVID-19-associated acute kidney injury: consensus report of the 25th Acute Disease Quality Initiative (ADQI) Workgroup. *Nat. Rev. Nephrol.* 2020;
20. Alexander MP, Mangalparthi KK, Madugundu AK, et al. Acute Kidney Injury in Severe COVID-19 Has Similarities to Sepsis-Associated Kidney Injury: A Multi-Omics Study. *Mayo Clin Proc* 2021;
21. Su H, Yang M, Wan C, et al. Renal histopathological analysis of 26 postmortem findings of patients with COVID-19 in China. *Kidney Int* 2020;
22. Farkash EA, Wilson AM, Jentzen JM. Ultrastructural evidence for direct renal infection with sars-cov-2. *J Am Soc Nephrol* 2020;
23. Klok FA, Kruip MJHA, van der Meer NJM, et al. Incidence of thrombotic complications in critically ill ICU patients with COVID-19. *Thromb Res* 2020;
24. Noris M, Benigni A, Remuzzi G. The case of complement activation in COVID-19 multiorgan impact. *Kidney Int.* 2020;
25. Al-Aly Z, Xie Y, Bowe B. High-dimensional characterization of post-acute sequelae of COVID-19. *Nature* 2021;
26. Bowe B, Xie Y, Xu E, Al-Aly Z. Kidney Outcomes in Long COVID. *J Am Soc Nephrol* 2021;
27. Shu T, Ning W, Wu D, et al. Plasma Proteomics Identify Biomarkers and Pathogenesis of COVID-19. *Immunity* 2020;

28. Park J, Kim H, Kim SY, et al. In-depth blood proteome profiling analysis revealed distinct functional characteristics of plasma proteins between severe and non-severe COVID-19 patients. *Sci Rep* 2020;
29. Su C-Y, Zhou S, Gonzalez-Kozlova E, et al. Circulating proteins to predict adverse COVID-19 outcomes. *medRxiv [Internet]* 2021;2021.10.04.21264015.
Available from:
<http://medrxiv.org/content/early/2021/10/05/2021.10.04.21264015.abstract>
30. Ferkingstad E, Sulem P, Atlason BA, et al. Large-scale integration of the plasma proteome with genetics and disease. *Nat Genet* 2021;
31. Yang J, Brody EN, Murthy AC, et al. Impact of kidney function on the blood proteome and on protein cardiovascular risk biomarkers in patients with stable coronary heart disease. *J Am Heart Assoc* 2020;
32. Gold L, Walker JJ, Wilcox SK, Williams S. Advances in human proteomics at high scale with the SOMAscan proteomics platform. *N Biotechnol* 2012;
33. Yu LR, Sun J, Daniels JR, et al. Aptamer-Based Proteomics Identifies Mortality-Associated Serum Biomarkers in Dialysis-Dependent AKI Patients. *Kidney Int Reports* 2018;
34. Charney AW, Simons NW, Mouskas K, et al. Sampling the host response to SARS-CoV-2 in hospitals under siege. *Nat. Med.* 2020;
35. Del Valle DM, Kim-Schulze S, Huang HH, et al. An inflammatory cytokine signature predicts COVID-19 severity and survival. *Nat Med* 2020;
36. Khwaja A. KDIGO clinical practice guidelines for acute kidney injury. *Nephron - Clin. Pract.* 2012;

37. Williams SA, Kivimaki M, Langenberg C, et al. Plasma protein patterns as comprehensive indicators of health. *Nat Med* 2019;
38. Kim CH, Tworoger SS, Stampfer MJ, et al. Stability and reproducibility of proteomic profiles measured with an aptamer-based platform. *Sci Rep* 2018;
39. Ritchie ME, Phipson B, Wu D, et al. Limma powers differential expression analyses for RNA-sequencing and microarray studies. *Nucleic Acids Res* 2015;43(7):e47.
40. Kuznetsova A, Brockhoff PB, Christensen RHB. lmerTest Package: Tests in Linear Mixed Effects Models . *J Stat Softw* 2017;
41. Szklarczyk D, Gable AL, Lyon D, et al. STRING v11: Protein-protein association networks with increased coverage, supporting functional discovery in genome-wide experimental datasets. *Nucleic Acids Res* 2019;
42. Doncheva NT, Morris JH, Gorodkin J, Jensen LJ. Cytoscape StringApp: Network Analysis and Visualization of Proteomics Data. *J Proteome Res* 2019;
43. Nugent J, Aklilu A, Yamamoto Y, et al. Assessment of Acute Kidney Injury and Longitudinal Kidney Function after Hospital Discharge among Patients with and without COVID-19. *JAMA Netw Open* 2021;
44. Basu RK, Wong HR, Krawczeski CD, et al. Combining functional and tubular damage biomarkers improves diagnostic precision for acute kidney injury after cardiac surgery. *J Am Coll Cardiol* 2014;
45. Nickolas TL, Schmidt-Ott KM, Canetta P, et al. Diagnostic and prognostic stratification in the emergency department using urinary biomarkers of nephron damage: A multicenter prospective cohort study. *J Am Coll Cardiol* 2012;

46. Du TY, Luo HM, Qin HC, et al. Circulating serum trefoil factor 3 (TFF3) is dramatically increased in chronic kidney disease. *PLoS One* 2013;
47. Madsen J, Nielsen O, Tornøe I, Thim L, Holmskov U. Tissue localization of human trefoil factors 1, 2, and 3. *J Histochem Cytochem* 2007;
48. Kjellev S. The trefoil factor family - Small peptides with multiple functionalities. *Cell. Mol. Life Sci.* 2009;
49. Astor BC, Köttgen A, Hwang SJ, Bhavsar N, Fox CS, Coresh J. Trefoil factor 3 predicts incident chronic kidney disease: A case-control study nested within the Atherosclerosis Risk in Communities (ARIC) study. *Am J Nephrol* 2011;
50. Chen Z, Hu J, Liu L, et al. SARS-CoV-2 Causes Acute Kidney Injury by Directly Infecting Renal Tubules. *Front Cell Dev Biol* 2021;
51. Lin W, Fan J, Hu LF, et al. Single-cell analysis of angiotensin-converting enzyme II expression in human kidneys and bladders reveals a potential route of 2019 novel coronavirus infection. *Chin Med J (Engl)* 2021;

Fig 1A

Fig 1A: Prospective cohort of patients enrolled between March 2020 – Aug 2020

Fig 1B: Timeline of measurements taken

Mount Sinai Discovery Cohort

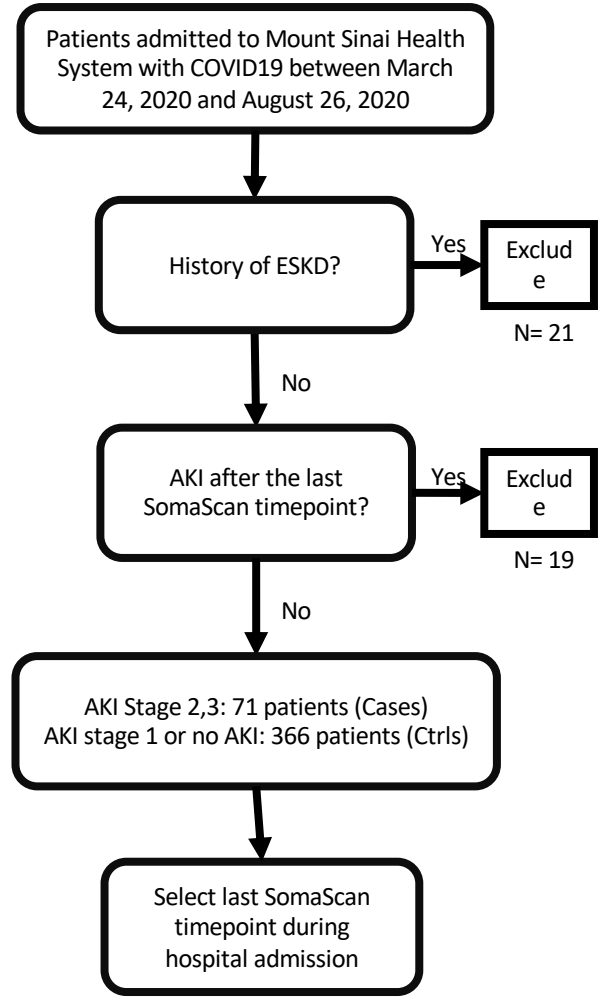


Fig 1B

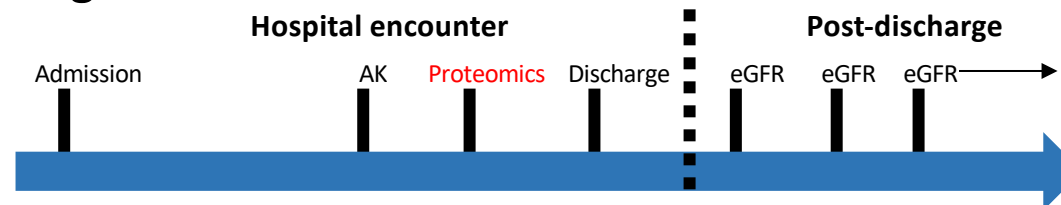


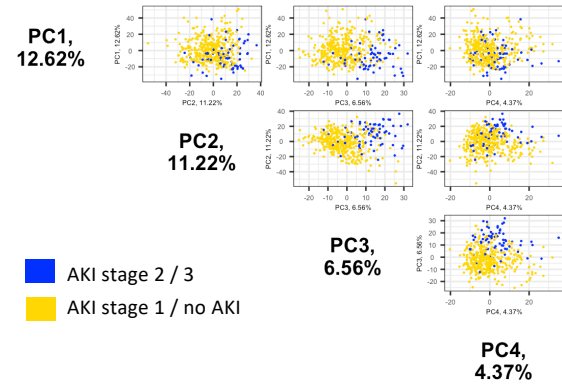
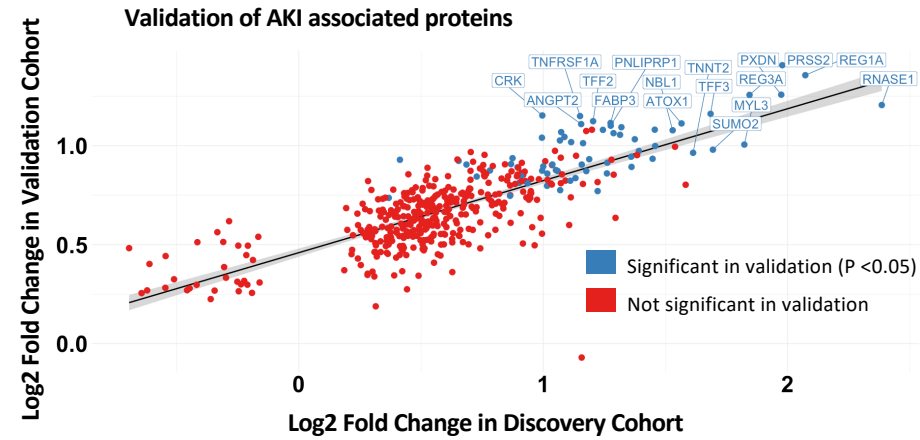
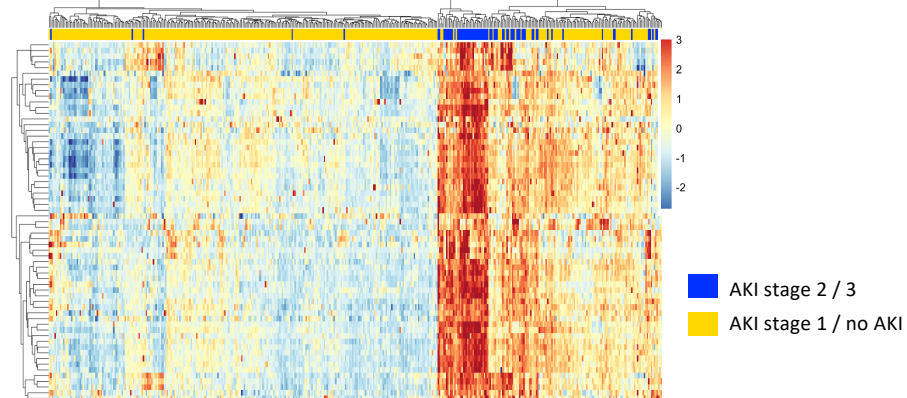
Fig 2**Principal component analysis of protein expression in discovery cohort****A****B****C****Expression of 62 protein AKI signature in discovery cohort**

Fig 3 Results Overview

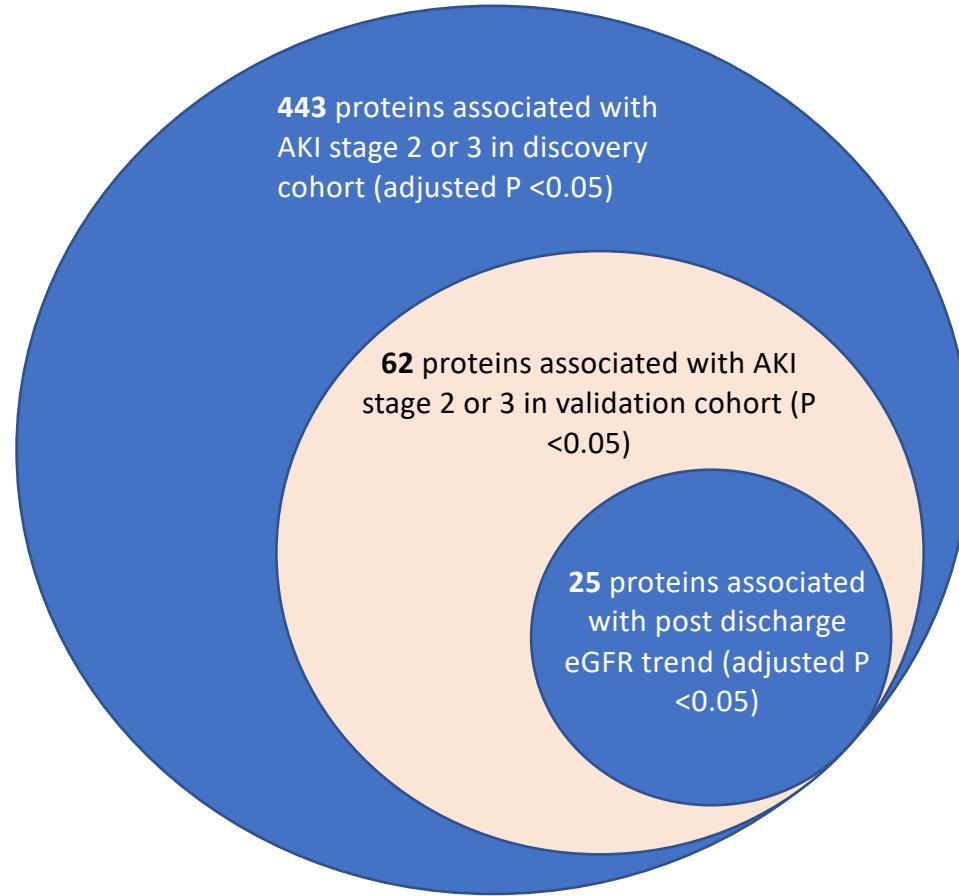
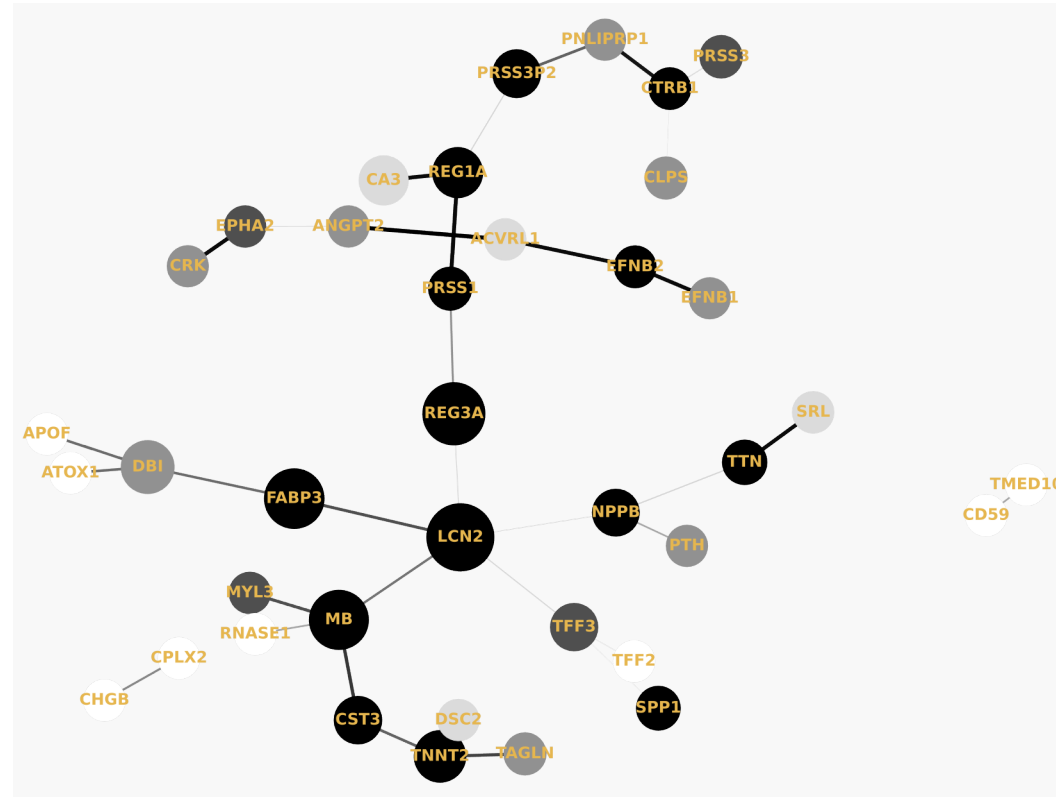


Fig 4

A

AKI associated protein-protein interaction network



B

Cardiac structure protein network

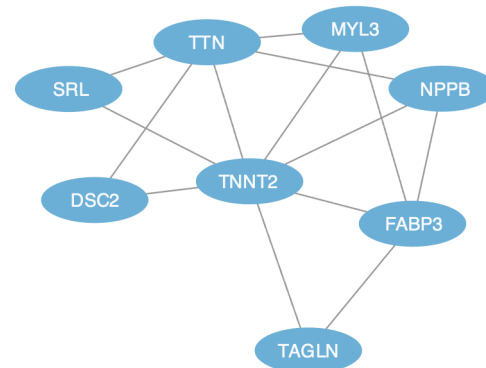
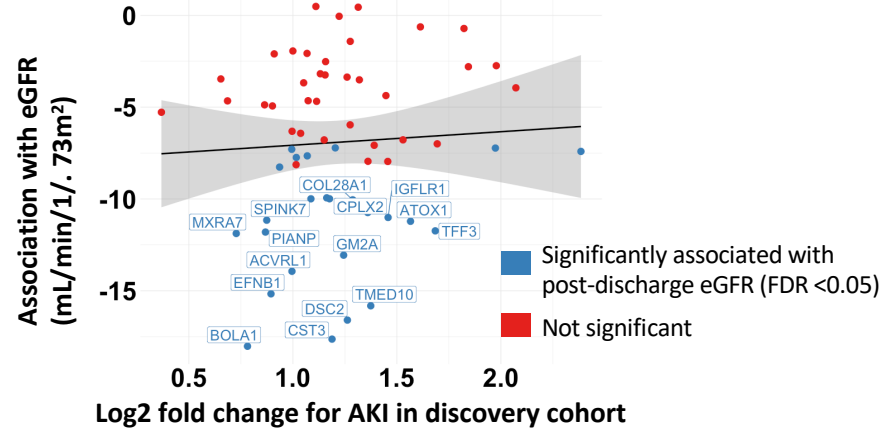


Fig 5 Proteomic characterization of post-discharge kidney function

A



B Protein expression

■ Top tertile ■ Middle tertile ■ Bottom tertile

